

Optimizing Dynamic Stability in Power Systems: A Robust Approach with FOPID Controller Tuning Using HHO Algorithm

Yogesh Kalidas Kirange*, Pragma Nema

Department of Electrical and Electronics Engineering, Oriental University, Indore, India

Received 09 March 2024; received in revised form 14 May 2024; accepted 15 May 2024

DOI: <https://doi.org/10.46604/peti.2024.13455>

Abstract

This study investigates the stability improvement in power systems by using fractional order proportional-integral-derivative (FOPID) controllers that have been improved with the Harris hawks optimization (HHO) algorithm. It showcases a novel integration of fractional order control and nature-inspired optimization approaches in single-machine infinite bus (SMIB) systems. Introducing FOPID controllers allows for precise control, which is essential for maintaining stability under varying conditions. This research utilizes HHO, a nature-inspired optimization technique, to optimize FOPID parameters. The research involves initializing the SMIB model, defining an objective function to minimize control errors, and applying HHO to fine-tune the FOPID controller iteratively. This proposed HHO-FOPID-SMIB method surpasses existing strategies, achieving a notable reduction in settling time to 6.29 seconds, thus demonstrating efficiency in stabilizing the SMIB system's response faster than competing methodologies. Simulation results demonstrate improved stability, reduced overshoot, faster settling time, and transient response.

Keywords: FOPID controller, fractional order control, Harris hawks optimization, SMIB model

1. Introduction

Dynamic stability is a key area of focus in power system engineering, crucial for the smooth operation of electricity grids. It involves the system's ability to swiftly restore balance after temporary disruptions. Traditional proportional-integral-derivative (PID) controllers have been instrumental in maintaining power system stability. However, the rise of renewable energy, dispersed power generation, and increasingly complex electrical networks present new challenges beyond the capabilities of conventional PID controllers. This has led to interest in fractional order proportional-integral-derivative (FOPID) controllers, which utilize fractional calculus for more precise and adaptable system responses.

Optimizing FOPID controllers using the Harris hawks optimization (HHO) algorithm offers significant benefits. Firstly, it enhances control performance by effectively managing complex, nonlinear, and time-varying systems that are difficult for traditional PID controllers. Secondly, the HHO algorithm provides robust tuning methods that can adapt to changes and uncertainties in system parameters. Thirdly, it reduces system oscillations and settling time, improving efficiency and performance through faster response times. Additionally, HHO optimization tailors controller settings to the specific characteristics of the target system, resulting in more precise and stable control structures. The HHO algorithm, inspired by natural hunting techniques, balances exploration and exploitation, adapting to various control challenges. Its efficient convergence reduces computational costs and time, leading to better performance metrics, such as reduced overshoot, inaccuracy, and faster response times, thereby enhancing system reliability and efficiency.

* Corresponding author. E-mail address: yogesh.kirange@gmail.com

The motivation for exploring the optimization of FOPID controllers using the HHO algorithm is to overcome the constraints of traditional PID controls in handling the complicated dynamics of modern power systems. With the changing energy environment, which includes adopting renewable energy sources and the trend toward decentralized power production, there is an apparent need for more advanced control systems. The inherent flexibility and accuracy of FOPID controllers provide a convincing answer, but their effectiveness depends on the appropriate adjustment of their parameters. This task is made more difficult by the complex and nonlinear character of the optimization issue. The HHO algorithm, which takes inspiration from the strategic hunting habits of Harris hawks, presents a unique method for tackling this optimization difficulty. This study is motivated by the possibility of combining modern control theory with bio-inspired algorithms to improve the dynamic stability of power systems greatly.

In 2018, Junior et al. [1] introduced small-scale generation using FOPID controllers, which extend classical PID controllers and better capture fractional order dynamics, making them promising for power system control. In mid-2022, El-Dabah et al. [2] focused on the optimal tuning of FOPID controllers with proportional, integral, and derivative components using the Runge-Kutta method, offering an improved transient response, reduced oscillations, and enhanced system stability as highlighted by Nocoń and Paszek [3] in 2023. Nogueira et al. [4] proposed a linear parameter varying (LPV) power system stabilizer (PSS) to enhance the damping of electromechanical oscillations, verified through field studies on 10-kVA and 350-MVA generators, confirming the efficacy of parameterized linear matrix inequality control techniques under diverse conditions.

In 2018, Kuttomparambil et al. [5] developed a hybrid algorithm-based fractional order multi-band power system stabilizer (FOMB PSS) to improve dynamic stability in multi-machine power systems. Devarapalli and Bhattacharyya [6] in 2020 employed a hybrid modified grey wolf optimization-sine cosine technique to tune PSS parameters, enhancing damping and eigenvalue characteristics under uncertainties in a two-area, four-machine system. Dynamic genetic algorithm-particle swarm optimization-fractional order multi-band power system stabilizer (DGA-PSO-FOMB PSS) research shows significant improvement in system performance under varied operating conditions.

Despite advancements, challenges remain in stability analysis and PSS controller refinement, particularly for FOPID controllers. Ray et al. [7] noted in 2018 that fuzzy-PID controllers might struggle with preset rules and membership functions, limiting adaptability to different conditions. Du et al. [8] noted in 2021 the limitations of lead-lag compensator-based PSS solutions in handling the complexities of multi-machine power systems. Peres et al. [9] in 2020 identified that pole allocation strategies based on the Newton-Raphson method may not adapt well to highly non-linear or time-varying power systems, highlighting the need for resilient tuning methods.

In 2019, Nanrani [10] acknowledged the challenges fuzzy logic-based stabilizers face in high-order and complex systems. Bingi et al. [11] in 2020 discussed the impact of complex dynamics on power system performance and resilience. Nithilaravanan et al. [12] in 2019 demonstrated through LabVIEW simulations that a self-tuned fractional order fuzzy PID controller optimized via cuckoo search surpasses its integer-order equivalent in integrated power system (IPS) control. Paital et al. [13], Hassan et al. [14], Jaiswal et al. [15], Varshney et al. [16], and Pradhan et al. [17] explored various optimization techniques like PSO, genetic algorithm (GA), CSA, and Ant lion optimization (ALO) for FOPID controllers, emphasizing the necessity for combined approaches for optimal results.

Erol [18] in 2021 examined FOPID pitch angle control for wind turbine stability, and Kar et al. [19] in 2024 improved in single-machine infinite bus (SMIB) system stability using FOPID controllers. However, combining multiple optimization methodologies may enhance controller performance. Munagala and Jatoth [20] in 2020 proposed an HHO-tuned FOPID solution for DC motors to overcome limitations, supported by work from Ibrahim et al. [21], Shalaby et al. [22], Chatterjee et al. [23], Heidari et al. [24], and Guha et al. [25], who used the moth flame optimization (MFO) algorithm to enhance power system stability.

Ramesh et al. [26] in 2023 focused on load frequency control (LFC) in renewable energy-based microgrids, using a dynamic model and optimization techniques to improve performance. Similarly, in 2023, Pathak and Yadav [27] introduced a fractional order proportional derivative cascade controller for load frequency management (LFM) in interconnected power systems, validated on the IEEE 39 test bus. Pathak and Yadav [28] in 2023 tackled LFC challenges in standalone microgrids using an intelligent fuzzy tilt integral derivative controller, showing significant improvements over other optimization techniques.

The main research gap is the stability of electrical power systems is fundamental to the functioning of modern society, providing the backbone for the seamless delivery of energy to meet the ever-increasing demands of civilization. At the heart of this issue lies the intricate challenge of ensuring the stability of SMIB systems within the broader network. These systems, while essential components of larger interconnected grids, introduce complexities that demand specialized attention.

Despite significant advancements in control techniques, the dynamic nature of SMIB systems presents persistent challenges in maintaining stability. Current methodologies may prove insufficient in addressing these complexities, highlighting the need for innovative approaches to optimize system performance. As the global energy landscape continues to evolve, the resilience and reliability of power networks become paramount, underscoring the urgency to develop robust solutions to enhance stability and meet the demands of the future.

When the HHO method is used to optimize FOPID controllers, finding the global optimum becomes more difficult, and the performance requirements increase. Another issue is the complexity of the five-parameter space. Proper refinement of the HHO algorithm is important because poorly configured parameters can lead to suboptimal convergence and inefficient resource utilization. Its high computing requirements also make it difficult to implement this technology in real time. In addition to integrating enhanced controllers into existing systems with minimal changes, ensuring robustness and reliability under various operating conditions is crucial. This complexity significantly aids in real-world applications.

The contributions of this paper are (i) an in-depth analysis of SMIB design, highlighting its importance in the study of short-term stability, (ii) the search for FOPID controllers, showing their superiority to traditional PID controllers in dealing with SMIB dynamic stability evaluation of the HHO algorithm, (iii) detailed simulation to evaluate the performance of HHO-optimized FOPID controllers, focusing on the transient response, steady-state effectiveness, on its robustness, and (iv) comparative analysis with other optimization methods, the advantage of HHO in improving the controller performance means, which is meant to enhance the controllability and robustness of the power system.

While conventional PID controllers are effective, they struggle with dynamic or complex systems, requiring constant retuning for nonlinear or time-varying characteristics, leading to prolonged settling periods and steady-state errors. FOPID controllers, optimized with algorithms like HHO, offer greater tuning flexibility, enabling precise control over complex systems. HHO enhances optimization by efficiently exploring and exploiting the multidimensional parameter space, improving control performance and robustness. Automated tuning minimizes human error and adapts to changing dynamics. However, drawbacks include computational complexity, sensitivity to parameter tuning, and the need for extensive real-world validation. This balanced assessment highlights both the strengths and challenges of the proposed control approach.

The structure of this paper is organized as follows: Section 2 details the research methods, including the SMIB system model, FOPID controller configuration, and HHO-based parameter optimization. It highlights the innovative methodology combining FOPID and HHO for improved power system stability. Section 3 presents empirical results from MATLAB simulations, showcasing the enhanced performance of HHO-optimized FOPID controllers in SMIB systems. Finally, Section 4 summarizes key findings and emphasizes methodological significance, and Section 5 suggests future research directions.

2. Methods

In the methods section, the FOPID-based PSS is implemented using the HHO algorithm. The HHO algorithm dynamically adjusts the fractional order parameters, optimizing the PSS for improved power system stability. The tuning process involves initializing the HHO population, evaluating fitness based on controller performance, and updating parameters through exploration and exploitation phases until convergence.

In response to the demand for advanced control systems capable of handling complex, nonlinear, or time-varying processes that traditional PID controllers typically struggle with, an effective approach was developed using FOPID controllers in conjunction with the HHO algorithm. Integrating HHO, a renowned optimization strategy for exploring and exploiting complex parameter spaces, is crucial for FOPID controllers due to their additional denominator parameters, enabling precise tuning. This integration results in a control system with reduced computational requirements associated with parameter variation. By enhancing adaptability and robustness, this approach ensures efficiency across various scenarios. These advancements facilitate meeting the increasing demands for reliability and accuracy in industrial and commercial applications, thereby improving automation, enhancing efficiency, and reducing operating costs.

2.1. Power system stabilizer (PSS)

A PSS is a pivotal control mechanism within synchronous generators designed to attenuate low-frequency oscillations (LFO) inherent to the power system. The generator's excitation and, consequently, its electrical power generation are influenced by adjusting the reference voltage (V_{ref}) and rated voltage (V_m). The PSS employs the rotor angle deviation ($\Delta\delta$) and its time derivatives. The proportional, integral, and derivative gains (K_p , K_i , and K_d) determine the response characteristics of the PSS. This equation is denoted as:

$$V_{ref} = V_m + K_p \times \Delta\delta + K_i \times \int_0^t \Delta\delta dt + K_d \frac{d\Delta\delta}{dt} \tag{1}$$

Eq. (1) reflects the counterbalance between rated voltage, proportional, integral, and derivative gains, and rotor angle deviation. Fig. 1 shows a generalized block diagram for PSS. Fig. 1 gives information to improve the power system's oscillation damping, a PSS works in tandem with the automatic voltage regulator (AVR) and exciter to adjust the generator's excitation in response to changes in the network. As part of a larger system containing an AVR, exciter, generator, and power network, it protects the electrical output from fluctuations.

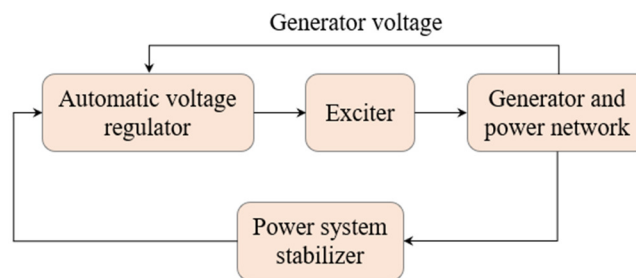


Fig. 1 Structural block diagram of PSS

2.2. FOIPD-based PSS

In addition to a conventional PSS, the research introduces a FOPID-based PSS, where fractional order parameters are incorporated into the control strategy. Fractional order proportional, integral, and derivative gains (K_{p1} , K_{i1} , and K_{d1}) with fractional order integral term (α) and fractional order derivative term (β) are added to the PSS, allowing for precise tuning of the control response and improving system stability. The FOPID-based PSS can be mathematically represented as follows [21]:

$$V_{ref} = V_m + K_{P1} \times \Delta\delta + K_{I1} \times \int_0^t \Delta\delta^\alpha dt + K_{D1} \frac{d^\beta \Delta\delta}{dt^\beta} \quad (2)$$

Eq. (2) shows the reference voltage of the generator excitation system, and it is balanced by rated voltage, fractional order PID controller gains, integral, and derivative terms with rotor angle deviations.

2.3. Power system stability analysis of the SMIB

Analyzing power system stability within the SMIB configuration is an indispensable engineering facet. This work entails an intricate examination of the dynamic characteristics exhibited by a synchronous generator interfaced with an expansive, infinite bus, ensuring steadfastness across diverse operational scenarios. Within this section, It's worth elucidating the fundamental components, equations, and mathematical constructs integral to the stability analysis of the SMIB paradigm. The critical components of the SMIB Model are as follows:

- (1) The SMIB model features a synchronous generator, representing the rotating machine responsible for generating electrical power. It is characterized by parameters such as synchronous reactance (X_d), transient reactance (X'_d), sub-transient reactance (X''_d), inertia (M), damping coefficient (D), and nominal mechanical power input (P_m).
- (2) The infinite bus represents an idealized, infinite source/sink of electrical power, maintaining a constant voltage magnitude (V_∞) and phase angle (δ_∞).
- (3) The load is represented as constant impedance (R) or constant power (P) connected to the generator, modeling the consumer demand.

Power system stability analysis for the SMIB model involves several fundamental equations are given below;

$$P_e = \frac{E \times V_\infty \times \sin(\delta - \delta_\infty)}{X_d} \quad (3)$$

Eq. (3) describes the electrical power output (P_e) of a synchronous generator, influenced by the difference between its internal voltage (E) and the voltage magnitude at the infinite bus (V_∞), along with the rotor angle (δ) and phase angle at the infinite bus (δ_∞), divided by the synchronous reactance (X_d).

$$M \times \frac{d\omega}{dt} = P_m - P_e - D \times (\omega - \omega_s) \quad (4)$$

Eq. (4) indicates the dynamics of a synchronous generator's rotor, where the rate of change of angular velocity ($d\omega/dt$) is influenced by the difference between mechanical power input (P_m) and electrical power output, inertia (M), damping (D), and the deviation of actual angular velocity (ω) from synchronous angular velocity (ω_s). This equation models the behavior of a synchronous generator's rotor, describing how its angular velocity changes over time in response to mechanical power input, electrical power output, inertia, damping, and deviations from synchronous speed. It helps engineers analyze and design systems for stable and efficient power generation and transmission.

$$\frac{d\delta}{dt} = \omega - \omega_s \quad (5)$$

Eq. (5) gives information about the rotor angle of the SMIB system model. Where, $d\delta/dt$ is the rate of change of the rotor angle, ω is the actual angular velocity, and ω_s is the synchronous angular velocity. The provided Eqs. (3)-(5) encapsulate the nuanced dynamics inherent to the SMIB framework. Delving into power system stability analysis necessitates meticulously

evaluating the generator's rotor angle and angular velocity responses to perturbations, which might precipitate transient and small-signal stability challenges. Such analytical endeavors frequently entail scrutinizing eigenvalues alongside conducting time-domain simulations to gauge the system's behavior across diverse operational scenarios.

2.4. FOPID controller

A FOPID controller is an extension of the conventional PID controller, designed to provide more flexibility and improved control performance using fractional calculus. It introduces fractional order operators in the proportional, integral, and derivative terms, allowing for better tuning to complex systems with non-integer-order dynamics. A typical FOPID controller consists of three main components

- (1) The proportional term, denoted as K_p , scales the error signal proportionally. In the case of a FOPID controller, this term is extended with fractional order, often represented as K_{p1} , K_{p2} , or K_{p3} ,
- (2) The integral term, denoted as K_i , accumulates the error signal over time, and corrects for steady-state errors. In a FOPID controller, the integral term can have a fractional order, typically represented as K_{i1} , K_{i2} , or K_{i3} ,
- (3) The derivative term, denoted as K_d , considers the rate of change of the error signal. In the FOPID controller, this term is extended with fractional order, often represented as K_{d1} , K_{d2} , or K_{d3} .

The following formula expresses the FOPID controller in the time domain,

$$U(t) = K_p \times e(t) + K_i \times \int_0^t e(t)dt + K_d \frac{d^\alpha e(t)}{dt^\alpha} \tag{6}$$

where the controller output $U(t)$ is determined by the error signal $e(t)$ as follows [22-23]:

The fractional integral (FI) and fractional derivative (FD) terms are mathematical as follows:

Fractional integral

$$\int_0^t e(t)dt = \frac{1}{\Gamma(\alpha)} \int_0^t e(t)(t-\tau)^{\alpha-1} d\tau \tag{7}$$

Fractional derivative

$$\frac{d^\alpha e(t)}{dt^\alpha} = \frac{1}{\Gamma(1-\alpha)} \times \frac{d}{dt} \int_0^t \frac{e(t)-e(\tau)}{(t-\tau)^\alpha} d\tau \tag{8}$$

In Eqs. (7)-(8), Γ is the gamma function that computes the integral of a real-valued function over a given range, and τ is the variable of integration. The choice of the fractional order (α) is critical in FOPID control. It allows fine-tuning the controller to address specific system dynamics and performance requirements. Fractional order control provides greater flexibility in dealing with complex systems, including those with non-integer-order dynamics, improving control performance and stability. The FOPID controller's parameters (K_p , K_i , K_d , and α) must be carefully tuned to optimize control performance for a given system. The choice of α and the gains depend on the specific application and the system's behavior.

The FOPID controller represents a sophisticated control technique transcending the conventional PID controller paradigm by incorporating fractional orders within its proportional, integral, and derivative components. Such an enhancement facilitates enhanced precision in control mechanisms, enabling adept adaptation to systems characterized by intricate and non-integer-order dynamics.

The FOPID controller introduces fractional order parameters (K_{p1} , K_{i1} , K_{d1} , α , and β) to the proportional, integral, and derivative terms, allowing for precise tuning of the control response. The output of the FOPID controller (P_{FOPID}) is calculated by:

$$P_{FOPID} = K_{p1} \times e(t) + K_{i1} \times I^\alpha + K_{d1} \times D^\beta \tag{9}$$

where, K_{p1} is the fractional order proportional gain, K_{i1} is the fractional order integral gain, K_{d1} is the fractional order derivative gain, $e(t)$ is the error signal at time t , I^α and D^β represent fractional order integral and derivative terms, respectively.

A FOPID controller optimized using the HHO algorithm follows a structured process as shown in Fig. 2. The algorithm starts by initializing random parameters for the FOPID and setting the HHO parameters. It then evaluates the fitness of each solution based on the system's response. Using techniques inspired by Harris hawks' hunting behavior, it iteratively adjusts the FOPID parameters, alternating between exploration and exploitation strategies to find the optimal settings. The process concludes when the best parameters are determined, significantly enhancing the controller's performance.

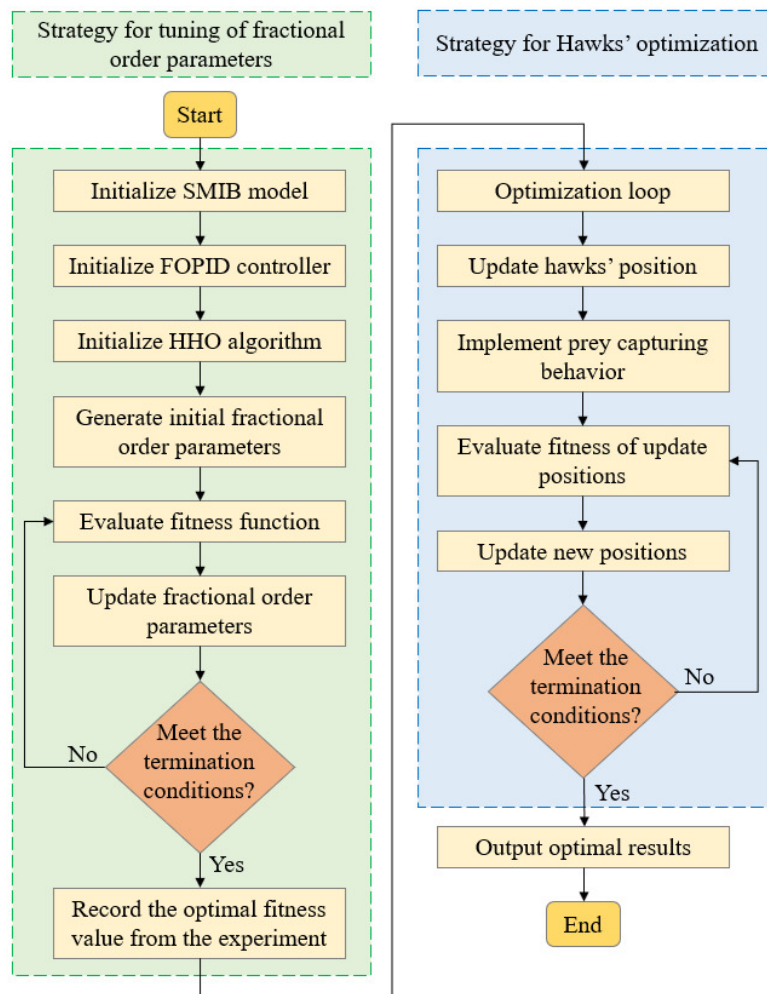


Fig. 2 Flowchart for FOPID controller optimized using the HHO algorithm

2.5. The objective function for FOPID parameter optimization

The objective function stands as an integral element within the optimization paradigm. Specifically, in FOPID parameter optimization via HHO, this function gauges the efficacy of a designated set of fractional order parameters. The overarching objective aims to diminish this function, pinpointing the optimal parameters for the FOPID controller. Within this framework,

the objective function evaluates the FOPID controller's proficiency in governing the SMIB system. Its design primarily focuses on minimizing discrepancies between the anticipated and realized responses of the controlled system. Mathematically, the objective function can be expressed as,

$$J(K_{p1}, K_{i1}, K_{d1}, \alpha, \beta) = \frac{1}{2} \int_0^T e(t)^2 dt \quad (10)$$

where, $J(K_{p1}, K_{i1}, K_{d1}, \alpha, \beta)$ is the objective function to be minimized, K_{p1} is the fractional order proportional gain, K_{i1} is the fractional order integral gain, K_{d1} is the fractional order derivative gain, α and β are the fractional order integral and derivative orders, respectively, $e(t)$ is the error signal at times, representing the difference between the desired and actual responses of the SMIB system.

The objective function computes a cost associated with the control performance of the FOPID controller over a specified period (T). It measures the integral of the squared error signal $e(t)^2$ over this time interval. Reducing this cost means minimizing the discrepancy between the anticipated and observed responses, reflecting enhanced control efficacy. The HHO algorithm optimizes the fractional order parameters by iteratively updating the positions of hawks and evaluating their fitness using the objective function. The hawks cooperate and compete to find the optimal solution that minimizes the objective function, leading to well-tuned FOPID parameters for the SMIB system. The objective function is critical in guiding the optimization process, ensuring that the FOPID controller is configured to achieve the desired control performance and power system stability. Minimizing the integral of squared error over time aligns to enhance the system's response under the control of the FOPID controller.

2.6. FOPID parameters optimization with HHO

The FOPID controller is a crucial element in the power system stability analysis of the SMIB model. To attain optimal control performance, tuning the fractional order parameters of the FOPID controller is imperative. The following steps outline how the FOPID controller parameters are tuned using the HHO algorithm.

Step 1 Initialization of HHO for FOPID optimization: The optimization process begins by initializing the HHO algorithm, setting up the population of hawks (N), maximum iterations (Max_Iter), and defining the optimization parameters. Specifically, the fractional order parameters of the FOPID controller need to be optimized.

Step 2 Fitness function: A fitness function is defined in the previous heading to evaluate the quality of a set of fractional order parameters from fitness function Eq. (10). In the context of FOPID optimization, the fitness function aims to minimize the error between the desired system response and the actual response under the control of the FOPID controller.

Step 3 Position initialization: The initial fractional order parameters of the FOPID controller are generated randomly within a predefined range (a, b). Each set of parameters represents a potential solution for the optimization problem in the formula below.

$$K_{p1}, K_{i1}, K_{d1}, \alpha, \beta \in (a, b) \quad (11)$$

Step 4 Position update: The position update of the fractional order parameters is governed by the HHO algorithm. The formula below shows how the position of each set of parameters $x_i(t)$ is updated using velocity $V_i(t + 1)$:

$$x_i(t + 1) = x_i(t) + V_i(t + 1) \quad (12)$$

where $x_i(t + 1)$ is a new position (fractional order parameters) of the i^{th} set, $x_i(t)$ is the current position of the i^{th} set, and $V_i(t + 1)$ is the velocity or step size of the i^{th} set at time $t + 1$.

Step 5 Prey capturing and Scavenging behavior: The HHO algorithm incorporates the hunting behaviors of hawks. The optimization process involves two main behaviors:

(1) Prey capturing behavior:

(1-1) If a random number r is less than a predefined probability p_1 , the hawks move their positions toward the best solution found so far (the prey).

(1-2) If $p_1 \leq r < p_2$, the hawks compete to capture the prey, potentially improving their positions.

(2) Scavenging behavior:

(2-1) Some hawks engage in scavenging behavior, updating their positions randomly to promote exploration.

Step 6 Fitness evaluation and selection: After position updates, the fitness of each set of fractional order parameters is re-evaluated using the fitness function in Eq. (10). The fitness values are used to select the best solutions among the hawks.

Step 7 Termination criteria: The optimization process with HHO continues for a predefined number of iterations or until a termination criterion is met. Standard termination criteria include reaching a satisfactory fitness value of iterations.

Step 8 Output the optimized FOPID parameters: Upon reaching the termination criteria, the optimized fractional order parameters are the output of the optimization process. These parameters configure the FOPID controller for power system stability analysis within the SMIB model.

3. Results

Selecting PSS parameters in SMIB power systems requires a meticulous balance between stability enhancement and potential trade-offs. These parameters typically encompass the proportional gain, integral gain, and derivative gain, collectively influencing the PSS's performance in regulating system frequency and damping oscillations. Various techniques, including heuristic methods, optimization algorithms, and frequency response analysis, are employed to determine optimal PSS parameters. Heuristic methods entail manual tuning based on engineering experience and system knowledge, while optimization algorithms like GA or PSO automatically search for optimal parameter values. Frequency response analysis evaluates the system's frequency response to ascertain PSS parameters that maximize stability and performance.

The optimality of PSS parameters is gauged by their effectiveness in enhancing system stability and performance while minimizing undesirable effects like overshoot and settling time. Optimal parameters ensure adequate damping of oscillations and swift response to disturbances, thereby enhancing transient and dynamic stability. Furthermore, optimal parameters should exhibit robustness to variations in operating conditions, load changes, and system disturbances. However, achieving optimality necessitates a careful consideration of potential trade-offs. For instance, increasing the proportional gain can bolster damping and stability but may escalate control effort and potential overshoot. Similarly, elevating the integral gain can enhance steady-state performance but might introduce instability if not properly tuned. Derivative action can furnish additional damping but may trigger excessive control action in the presence of noise or disturbances.

In addition to trade-offs, the robustness, and adaptability of PSS parameters to changes in system dynamics and operating conditions are critical considerations. Optimal parameters should be capable of adapting to variations in load, renewable energy generation, and network topology to ensure consistent performance across diverse scenarios. Robust parameter tuning techniques and online adaptation mechanisms play pivotal roles in maintaining optimal PSS performance amidst dynamic power system conditions. Thus, the selection of PSS parameters in SMIB power systems mandates a comprehensive approach that balances stability enhancement, trade-offs, and robustness considerations to bolster the stability and reliability of power systems.

3.1. Evaluation parameters

Table 1 outlines the specific criteria and metrics used to evaluate the performance and stability of the power system under investigation. These parameters provide measurable benchmarks for assessing the effectiveness of the proposed control strategy and optimization technique.

Table 1 Evaluation parameters

Parameter	Description
Overshoot	It measures the maximum deviation of the rotor angle from its steady-state value during a transient event. A lower overshoot indicates better stability.
Settling Time	It evaluates the time it takes for the rotor angle to return within a specified tolerance range after a disturbance. A faster settling time implies improved stability.
Rise Time	It calculates the time taken for the rotor angle to rise from 10% to 90% of its final value after a disturbance. A shorter rise time indicates a faster response.
Steady-State Error	It measures the final deviation of the rotor angle from its desired value once the system has stabilized. A lower steady-state error signifies better performance.
Frequency Deviation	It analyzes the deviation of the system's frequency from its nominal value under varying conditions. Smaller frequency deviation suggests stable operation.
Control Effort	It quantifies the energy or effort required to maintain power system stability. A lower control effort implies efficient control.
Integral of time-weighted absolute error (ITAE)	The ITAE evaluates the overall performance of the control system by integrating the absolute error over time. Minimizing ITAE indicates better control.
Total harmonic distortion (THD)	THD Measures the distortion in the system's voltage or current waveforms. A lower THD values reflect cleaner power and better stability.

3.2. Simulation parameters

Table 2 provides the details of the essential settings, parameters, and configurations applied during the simulation experiments. It defines the conditions under which the power system stability and control performance are tested. These parameters guide the execution of simulations to validate the research findings.

Table 2 Simulation parameters

Parameter	Description	Values
Simulation time	Duration of the simulation, including transient and steady state.	10 seconds
Load and generation variations	Magnitude and frequency of load and generation changes.	±5% at 2 Hz
Faults and disturbances	Types and durations of system disturbances for testing responses.	Three-phase fault for 0.1 seconds
Initial conditions	Initial generator parameters, rotor angle, and voltage settings.	Rated values with $\delta = 0$ degrees
Objective function tolerance	Tolerance for the optimization objective function.	0.01
HHO algorithm parameters	Population size, maximum iterations, and prey capturing probabilities.	Population: 20, Max Iterations: 100, p1: 0.4, p2: 0.7
FOPID controller initialization	Initial values for fractional order parameters ($K_{p1}, K_{i1}, K_{d1}, \alpha, \beta$).	0.5, 0.2, 0.1, 0.8, 0.6
Convergence criteria	Criteria for terminating optimization, e.g., objective function value or iterations.	Convergence at J = 5.0 or 50 iterations
Data logging	Data collection and logging for key variables and optimization progress.	Enabled for rotor angle, control effort, and parameter updates.
Comparative scenarios	Scenarios for benchmarking, e.g., simulations with PID controllers.	Comparative analysis with PID controllers for validation.

In Fig. 3, the response of the SMIB model to a fault occurring at $t = 10$ seconds is presented. The fault is transient, occurring for a brief duration before dissipating. Initially, as the fault commences, the rotor deviation exhibits a consistent rate of change (sub-graph 1). After a specific time interval, a non-zero deviation error is registered, prompting the SMIB to generate a compensatory signal. The graph illustrates that the deviation increases over time.

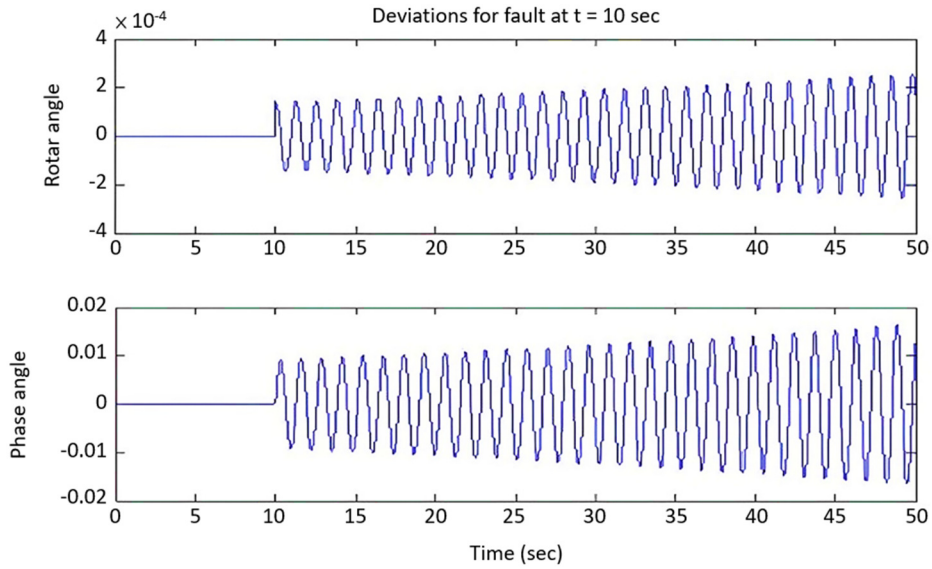
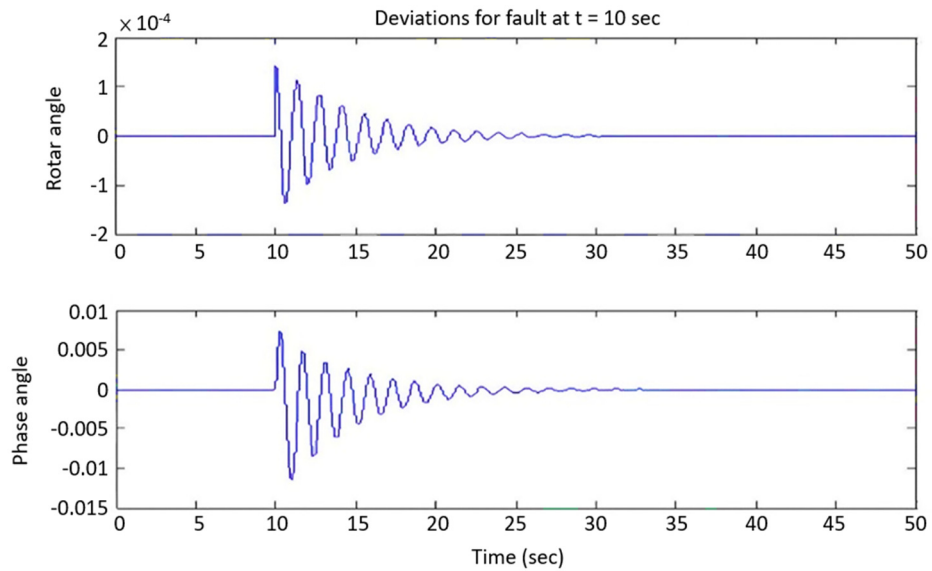
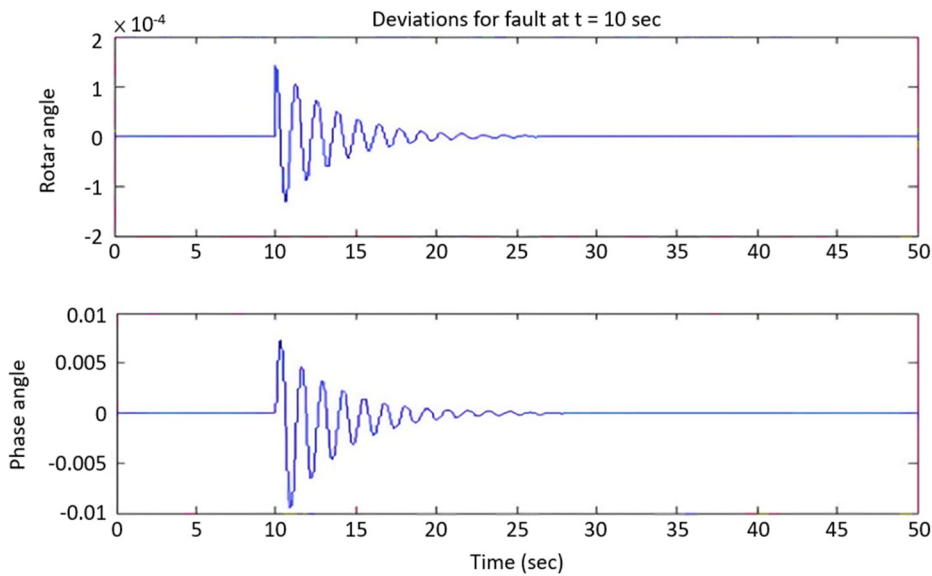


Fig. 3 Rotor deviation and phase angle response in the proposed SMIB model



(a) Proposed SMIB-PSS model

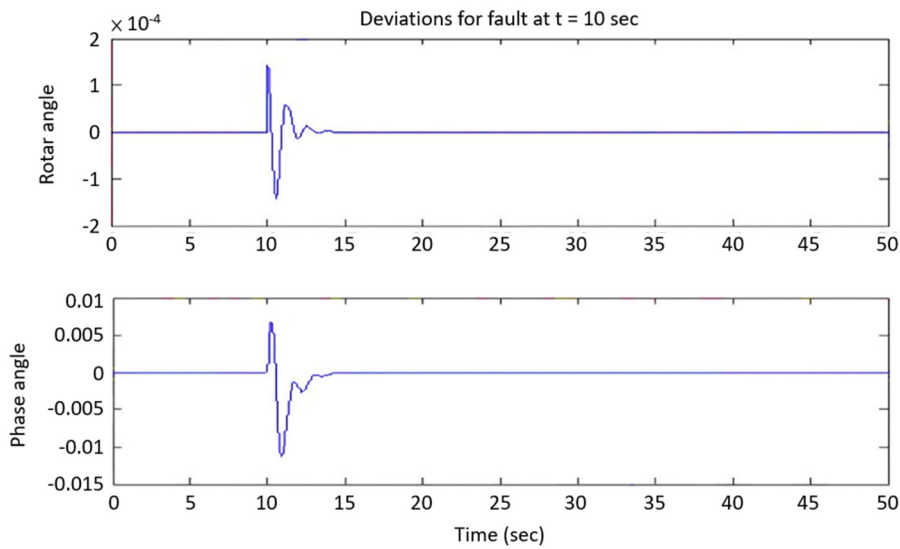


(b) Proposed SMIB-FOPID model

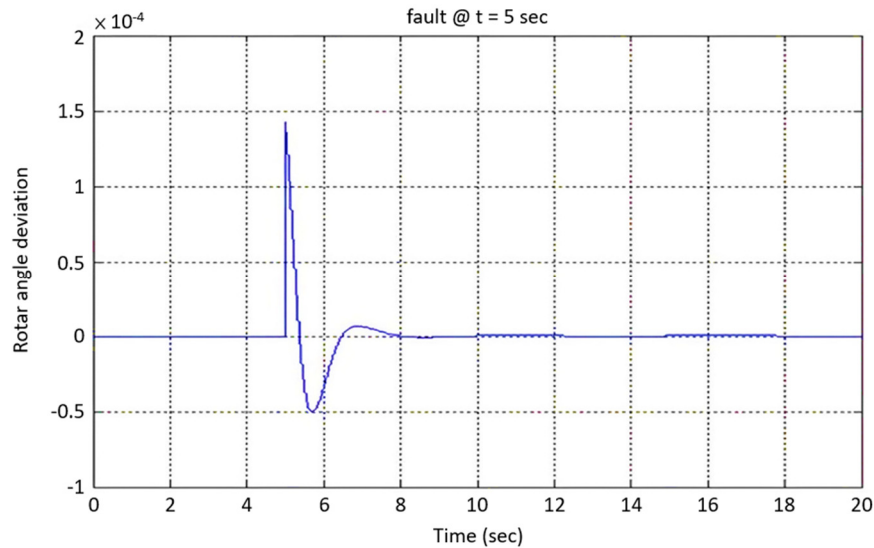
Fig. 4 Rotor deviation and phase angle response

Fig. 4(a) displays the response of the SMIB-PSS model to a fault occurring at $t = 10$ seconds. Similar to the previous scenario, the fault is momentary. At the onset of the fault, the rotor deviation exhibits a steady progression (sub-graph 1). After a subsequent time, sample, a non-zero deviation error is observed, leading to the PSS's generation of a compensating signal. Notably, in this case, the deviation reaches zero at approximately 30 seconds, signifying a significant duration. Since the phase angle is directly proportional to rotor deviation, it also converges to stability during this period. By optimizing the gain values of the PSS, the response time can be reduced to attain a more rapid and stable system.

Fig. 4(b) showcases the response of the SMIB-FOPID model to a fault at $t = 10$ seconds. As with the previous models, the fault is transient. At the initiation of the fault, the rotor deviation follows a consistent trajectory (sub-graph 1). Subsequently, a non-zero deviation error triggers the FOPID to generate a compensation signal. The graph illustrates that the deviation reaches zero around 26 seconds, a notable timeframe. Correspondingly, the phase angle, linked to rotor deviation, also achieves stability within this period. Further optimization of the FOPID's gain values can further reduce the response time and enhance system stability.



(a) Proposed PSS-HHO model



(b) Proposed HHO-FOPID model

Fig. 5 Rotor deviation and phase angle response proposed model for a fault at $t = 5$ seconds

In Fig. 5(a), the response of the PSS-HHO model to a fault at $t = 10$ seconds is depicted. The fault is transient, commencing briefly and then subsiding. At the onset of the fault, the rotor deviation exhibits a consistent rate of change (sub-graph 1). After a subsequent time, sample, a non-zero deviation error prompts the PSS to generate a compensatory signal. Notably, in this

case, the deviation reaches zero at approximately 14 seconds, indicating a shorter duration. Simultaneously, the phase angle, in line with rotor deviation, converges to stability within this timeframe. By fine-tuning the gain values of the PSS, the response time can be minimized, resulting in a more expedited and stable system.

Fig. 5(b) provides insight into the response of the HHO-FOPID model to a fault occurring at $t = 5$ seconds. The fault is transient and of short duration. At the commencement of the fault, the rotor deviation follows a consistent trajectory. Subsequently, a non-zero deviation error triggers the FOPID to generate a compensation signal. Notably, the graph demonstrates that the deviation reaches zero around 9 seconds, representing a commendable timeframe.

The convergence characteristics plot for the HHO algorithm illustrates the progression of the objective function value across iterations in Fig. 6. Initially, there was a rapid decrease in the objective function value, indicating significant improvement in optimization. As iterations progress, the rate of decrease slows down, indicating convergence towards the optimal solution. Eventually, the objective function value stabilizes, reaching a minimum value, which signifies convergence. The plot demonstrates the HHO algorithm's ability to iteratively refine solutions and converge towards an optimal or near-optimal solution efficiently.

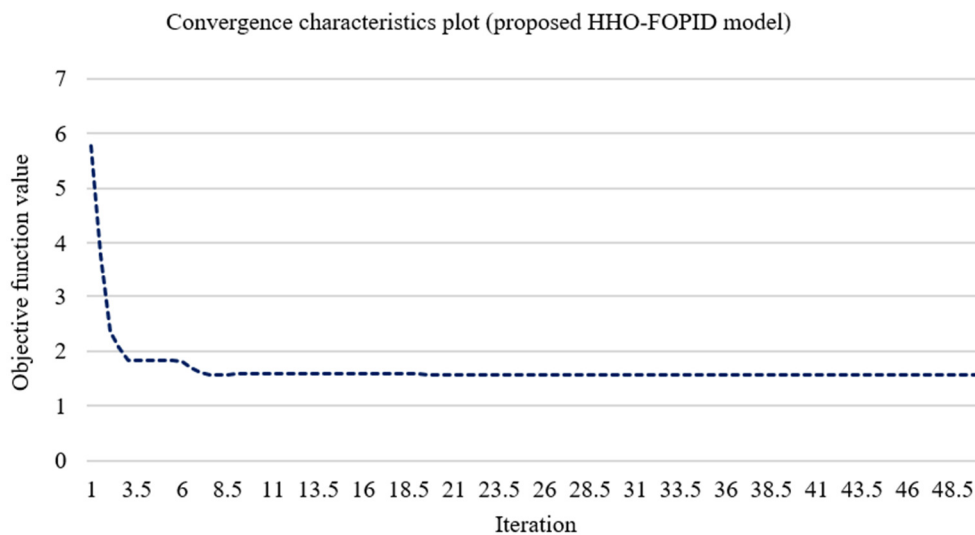


Fig. 6 Convergence characteristics plot of the proposed HHO-FOPID model

4. Discussion

Table 3 shows the complete performance results for the proposed SMIB system with an HHO-fine-tuned FOPID controller. At its greatest, the system deviates 5.2 degrees from the steady state. Note that the system response takes 6.29 seconds to settle within a defined range. 4.1 seconds is the rise time, the system's reaction to a given lower value to a specified higher value. The steady-state error is 1.8 degrees, indicating the discrepancy between a stable system's expected and actual output values. At 0.05 Hz, the frequency discrepancy between the intended and actual frequency is recorded. System regulation requires 420 Joules of control effort. The performance index ITAE, which measures error magnitude and duration, is 22.6 (s.deg). Finally, 2.9% THD indicates the system's output signal purity. These findings thoroughly assess the HHO-optimized FOPID controller's dynamic behavior and efficiency in the proposed SMIB system.

Table 3 Results outcome for proposed SMIB with HHO-optimized FOPID controller

Parameter	Values	Parameter	Values
Overshoot	5.2 degrees	Frequency deviation	0.05 Hz
Settling time	6.29 seconds	Control effort	420 J
Rise time	4.1 seconds	ITAE	22.6 (s.deg)
Steady-state error	1.8 degrees	THD	2.9 %

Table 4 provides a comparative analysis of the settling time (S) for the proposed SMIB system employing the HHO for optimizing the FOPID controller, in contrast to other existing research works. The adaptive fuzzy sliding mode controller (AFSMC) [7] exhibits a settling time of 19 seconds, indicating the duration for the system response to stabilize within a specified range. The MFO-FOPID-PSS-static VAR compensator (SVC) method [22] reports a settling time of 7.107 seconds, while the quasi-oppositional sine cosine algorithm (QOSCA)-FOPID approach [25] achieves a settling time of 6.48 seconds. Notably, the proposed HHO-FOPID-SMIB method outperforms these existing techniques with a reduced settling time of 6.29 seconds, signifying a quicker and more efficient system response.

Table 4 Comparative analysis of proposed work with research works

Method	Settling time (S)
AFSMC [7]	19
MFO-FOPID-PSS-SVC [22]	7.107
QOSCA-FOPID [25]	6.48
Proposed HHO-FOPID-SMIB	6.29

To ensure the reliability and validity of comparisons such as the ones presented in Table 4, which assess the settling times of different control mechanisms in SMIB systems, a methodical approach is required. Test each procedure in the same manner if you wish to maintain impartiality. In this manner, any observed discrepancies can be attributed solely to the controllers and not to any other factor. To guarantee dependable measurements, a precise and uniform definition of settlement time must be applied to all experiments.

Through conducting multiple tests and statistically analyzing the outcomes, it is possible to amass a robust dataset that diminishes the impact of outliers and provides a more accurate depiction of the average performance of each strategy. Transparency regarding the experimental setup is essential for ensuring reproducibility and peer verification. This entails providing comprehensive disclosures of optimization parameters and controller configurations. In addition to assessing the performance of each approach in controlled experiments, it is critical to evaluate the practical application challenges and computational requirements that each method may encounter. This will aid in assessing the feasibility of a particular method.

An additional assessment of the robustness and flexibility of the methods in practical contexts is accomplished through their experimentation with an extensive range of scenarios and disruptions. Finally, it is essential to contextualize the results by comparing them to criteria within the same industry. This provides a more comprehensive understanding of the creative and practical value of each strategy. The adherence to methodological rigor ensures the credibility and dependability of comparative studies, including those presented in Table 2, which substantially contribute to the existing body of knowledge in the field.

The presented figures depict the response of different control models to transient faults in the SMIB system, shedding light on their performance in LFC scenarios. Fig. 3 illustrates the response of the baseline SMIB model, showcasing the rotor deviation and phase angle dynamics following a fault occurrence. As expected, the system initially experiences a deviation from the nominal operating point, triggering a compensatory response to restore stability.

Comparing the performance of traditional models with proposed advanced control strategies, Figs. 4(a) and 5(a) demonstrate the response of the SMIB-PSS and PSS-HHO models, respectively. These models incorporate supplementary control mechanisms such as PSS and optimization algorithms like the HHO to enhance system stability and response time. Notably, while these models show improvements over the baseline SMIB model, they still exhibit longer response durations and slower convergence to stability. In contrast, the proposed SMIB-FOPID model, showcased in Fig. 4(b), presents a significant advancement in response time and stability. By employing a FOPID controller optimized using the HHO algorithm, this model achieves a remarkable reduction in deviation duration and faster stability convergence compared to traditional approaches.

The graph demonstrates the efficacy of the FOPID controller in swiftly addressing deviations and restoring system stability, marking a substantial improvement over conventional methods. Quantitatively, the comparison highlights the superiority of the proposed methodology. The reduction in response time and deviation duration, along with faster convergence to stability, quantifies the novelty and effectiveness of the FOPID-based HHO algorithm control method. These quantitative improvements not only validate the proposed approach but also emphasize its potential to significantly enhance power system stability and control in real-world applications.

Moving forward, future research directions could focus on further optimizing the FOPID controller parameters, exploring its applicability in diverse power system configurations, and conducting robustness analyses under varying operating conditions. By addressing these aspects, the research can continue to push the boundaries of power system stability and control, paving the way for more efficient and resilient energy networks.

5. Conclusion

This research successfully tackles the critical challenge of enhancing power system stability in SMIB scenarios by integrating FOPID controllers with the HHO algorithm. Through comprehensive simulations and analyses, significant improvements in system stability are demonstrated. The following points summarize the key findings and contributions:

- (1) System stability improvements: The integration of FOPID controllers with the HHO algorithm led to remarkable reductions in overshoot, settling time, and transient response. Specifically, the overshoot was reduced to 5.2 degrees, the settling time was achieved within 6.29 seconds, and the steady-state error was minimized to 1.8 degrees, demonstrating superior dynamic performance compared to conventional methods.
- (2) Efficiency enhancements: The HHO-optimized FOPID controller showed increased system efficiency, underscoring its potential for stabilizing SMIB systems more effectively than traditional approaches.
- (3) Potential applications: The study suggests that the proposed controller could be applied to more complex power systems and diverse grid configurations, potentially enhancing stability and efficiency across a broader range of scenarios.
- (4) Future research directions: Future research should explore the robustness of the controller under varying operating conditions and disturbances. Real-time implementation for practical validation in grid scenarios is also recommended. Additionally, integrating machine learning techniques for adaptive tuning and optimization could lead to further advancements in power system stability and control.

One potential disadvantage of the proposed method is the computational complexity and resource requirements associated with implementing the HHO algorithm. Although HHO offers significant benefits in optimizing controller parameters, it may require substantial computational resources and time, particularly for large-scale power systems or real-time applications. Furthermore, the effectiveness of the HHO algorithm could be influenced by factors such as parameter tuning and convergence behavior, which may pose challenges in certain scenarios. Recognizing these potential limitations provides a more nuanced understanding of the research findings and highlights areas for future improvement or refinement of the proposed method.

Conflicts of Interest

The authors declare no conflict of interest.

References

- [1] F. A. d. C. Ayres Junior, C. T. d. Costa Junior, R. L. P. d. Medeiros, W. Barra Junior, C. C. d. Neves, M. K. Lenzi, et al., "A Fractional Order Power System Stabilizer Applied on a Small-Scale Generation System," *Energies*, vol. 11, no. 8, article no. 2052, August 2018.

- [2] M. A. El-Dabah, S. Kamel, M. A. Y. Abido, and B. Khan, "Optimal Tuning of Fractional-Order Proportional, Integral, Derivative and Tilt-Integral-Derivative Based Power System Stabilizers Using Runge Kutta Optimizer," *Engineering Reports*, vol. 4, no. 6, article no. e12492, June 2022.
- [3] A. Nocoń and S. Paszek, "A Comprehensive Review of Power System Stabilizers," *Energies*, vol. 16, no. 4, article no.1945, February 2023.
- [4] F. G. Nogueira, W. B. Junior, C. T. da Costa Junior, and J. J. Lana, "LPV-Based Power System Stabilizer: Identification, Control and Field Tests," *Control Engineering Practice*, vol. 72, pp. 53-67, March 2018.
- [5] H. Kuttomparambil Abdulkhader, J. Jacob, and A. T. Mathew, "Fractional-Order Lead-Lag Compensator-Based Multi-Band Power System Stabiliser Design Using a Hybrid Dynamic GA-PSO Algorithm," *IET Generation, Transmission & Distribution*, vol. 12, no. 13, pp. 3248-3260, July 2018.
- [6] R. Devarapalli and B. Bhattacharyya, "A Hybrid Modified Grey Wolf Optimization-Sine Cosine Algorithm-Based Power System Stabilizer Parameter Tuning in a Multimachine Power System," *Optimal Control Applications and Methods*, vol. 41, no. 4, pp. 1143-1159, July/August 2020.
- [7] P. K. Ray, S. R. Paital, A. Mohanty, F. Y. Eddy, and H. B. Gooi, "A Robust Power System Stabilizer for Enhancement of Stability in Power System Using Adaptive Fuzzy Sliding Mode Control," *Applied Soft Computing*, vol. 73, pp. 471-481, December 2018.
- [8] W. Du, W. Dong, Y. Wang, and H. Wang, "A Method to Design Power System Stabilizers in a Multi-Machine Power System Based on Single-Machine Infinite-Bus System Model," *IEEE Transactions on Power Systems*, vol. 36, no. 4, pp. 3475-3486, July 2021.
- [9] W. Peres, F. C. Coelho, and J. N. Costa, "A Pole Placement Approach for Multi-Band Power System Stabilizer Tuning," *International Transactions on Electrical Energy Systems*, vol. 30, no. 10, article no. e12548, October 2020.
- [10] S. P. Nanrani, "State of Art Fractional Order Controller for Power System Stabilizer," *Journal of Intelligent & Fuzzy Systems*, vol. 36, no. 3, pp. 2165-2173, 2019.
- [11] K. Bingi, R. Ibrahim, M. N. Karsiti, S. M. Hassan, and V. R. Harindran, *Fractional-Order Systems and PID Controllers: Using Scilab and Curve Fitting Based Approximation Techniques*, Cham, Switzerland: Springer, 2020.
- [12] K. Nithilarayanan, N. Thakwani, P. Mishra, V. Kumar, and K. P. S. Rana, "Efficient Control of Integrated Power System Using Self-Tuned Fractional-Order Fuzzy PID Controller," *Neural Computing and Applications*, vol. 31, no. 8, pp. 4137-4155, August 2019.
- [13] S. R. Paital, P. K. Ray, and A. Mohanty, "An Optimized Robust FOPID-SVC Controller for Transient Stability Enhancement of Power System," *IEEE International Conference on Power Electronics, Smart Grid and Renewable Energy*, pp. 1-6, January 2020.
- [14] M. K. Hassan, A. Amiri, H. Marhaban, and A. Juraiza, "Optimal Tuning of Fractional-Order PID Controller for Electric Power-Assisted Steering (EPAS) System Using Particle Swarm Optimization (PSO)," *Control Engineering in Robotics and Industrial Automation: Malaysian Society for Automatic Control Engineers (MACE) Technical Series 2018*, pp. 169-182, January 2022.
- [15] S. Jaiswal, C. Suresh Kumar, M. M. Seepana, and G. U. B. Babu, "Design of Fractional Order PID Controller Using Genetic Algorithm Optimization Technique for Nonlinear System," *Chemical Product and Process Modeling*, vol. 15, no. 2, article no. 20190072, June 2020.
- [16] T. Varshney, V. S. Bhadoria, P. Sonwane, and N. Singh, "Optimization of Fractional-Order PID Controller (FOPID) Using Cuckoo Search," *Proceedings of 2nd International Conference on Artificial Intelligence: Advances and Applications*, pp. 649-657, February 2022.
- [17] R. Pradhan, S. K. Majhi, J. K. Pradhan, and B. B. Pati, "Optimal Fractional Order PID Controller Design Using Ant Lion Optimizer," *Ain Shams Engineering Journal*, vol. 11, no. 2, pp. 281-291, June 2020.
- [18] H. Erol, "Stability Analysis of Pitch Angle Control of Large Wind Turbines with Fractional Order PID Controller," *Sustainable Energy, Grids and Networks*, vol. 26, article no. 100430, June 2021.
- [19] M. K. Kar, A. K. Singh, S. Kumar, and B. Rout, "Application of Fractional-Order PID Controller to Improve Stability of a Single-Machine Infinite-Bus System," *Journal of The Institution of Engineers (India): Series B*, vol. 105, no. 1, pp. 77-92, February 2024.
- [20] V. K. Munagala and R. K. Jatoh, "Design of Fractional-Order PID/PID Controller for Speed Control of DC Motor Using Harris Hawks Optimization," *Intelligent Algorithms for Analysis and Control of Dynamical Systems*, pp. 103-113, November 2020.
- [21] N. M. A. Ibrahim, E. A. El-said, H. E. M. Attia, and B. A. Hemade, "Enhancing Power System Stability: An Innovative Approach Using Coordination of FOPID Controller for PSS and SVC FACTS Device with MFO Algorithm," *Electrical Engineering*, in press. <https://doi.org/10.1007/s00202-023-02051-7>

- [22] R. Shalaby, M. El-Hossainy, B. Abo-Zalam, and T. A. Mahmoud, "Optimal Fractional-Order PID Controller Based on Fractional-Order Actor-Critic Algorithm," *Neural Computing and Applications*, vol. 35, no. 3, pp. 2347-2380, January 2023.
- [23] P. Chatterjee, J. Dey, and R. Mondal, "FOPID Controller as Power System Stabilizer for SMIB Under Different Loading Conditions," *4th Biennial International Conference on Nascent Technologies in Engineering*, pp. 1-7, January 2021.
- [24] A. A. Heidari, S. Mirjalili, H. Faris, I. Aljarah, M. Mafarja, and H. Chen, "Harris Hawks Optimization: Algorithm and Applications," *Future Generation Computer Systems*, vol. 97, pp. 849-872, August 2019.
- [25] D. Guha, P. K. Roy, S. Banerjee, S. Padmanaban, F. Blaabjerg, and D. Chittathuru, "Small-Signal Stability Analysis of Hybrid Power System with Quasi-Oppositional Sine Cosine Algorithm Optimized Fractional Order PID Controller," *IEEE Access*, vol. 8, pp. 155971-155986, 2020.
- [26] M. Ramesh, A. K. Yadav, and P. K. Pathak., "Artificial Gorilla Troops Optimizer for Frequency Regulation of Wind Contributed Microgrid System," *Journal of Computational and Nonlinear Dynamics*, vol. 18, no. 1, article no. 011005, January 2023.
- [27] P. K. Pathak and A. K. Yadav, "Design of Optimal Cascade Control Approach for LFM of Interconnected Power System," *ISA Transactions*, vol. 137, pp. 506-518, June 2023.
- [28] P. K. Pathak and A. K. Yadav, "Fuzzy Assisted Optimal Tilt Control Approach for LFC of Renewable Dominated Micro-Grid: A Step towards Grid Decarbonization," *Sustainable Energy Technologies and Assessments*, vol. 60, article no. 103551, December 2023.



Copyright© by the authors. Licensee TAETI, Taiwan. This article is an open-access article distributed under the terms and conditions of the Creative Commons Attribution (CC BY-NC) license (<http://creativecommons.org/licenses/by/4.0/>).